Journal of Alloys and Compounds 509 (2011) 5903–5907

Contents lists available at ScienceDirect

Journal of Alloys and Compounds

journal homepage: www.elsevier.com/locate/jallcom

Influence of ZnO content and annealing temperature on the dielectric properties of ZnO/Al_2O_3 composite coatings

Liang Zhou*, Wancheng Zhou, Tao Liu, Fa Luo, Dongmei Zhu

State Key Laboratory of Solidification Processing, Northwestern Polytechnical University, Xi'an 710072, China

ARTICLE INFO

Article history:
Received 5 November 2010
Received in revised form 1 March 2011
Accepted 2 March 2011

PACS:
81.15.Rs, 81.40.Rs, 77.22.Ch, 78.20.Ci

Keywords:
Plasma spraying
Dielectric properties
Radar absorbing coating
Zinc oxide

ABSTRACT

ZnO/Al_2O_3 coatings were prepared by atmospheric plasma spraying (APS) using ZnO powders and Al_2O_3 powders as starting materials. The dielectric properties of these coatings were discussed. Both the real part of permittivity and the energy loss increase greatly with increasing ZnO content over the frequency range 8.2–12.4 GHz, which can be ascribed to orientation polarization and relaxation polarization due to a higher ZnO content. The frequency-dependent maximum of the loss tangent is found to obey Debye theory. In addition, annealing temperature which leads to the change of ZnO content also plays an important role in the dielectric performance.

1. Introduction

Because of the wide band gap (3.3 eV), excellent chemical and thermal stability, and specific electrical and optoelectronic properties of being a II–VI compound semiconductor, Zinc oxide (ZnO) has attracted much research attention [1]. Owing to these, a broad range of high-technology applications, including photo catalysts [2], photonic crystals [3], light emitting diodes [4], transparent conductors [5,6], optical modulator waveguides [7], gas sensors [8], and solar cells [9] are based on this material. And various techniques such as chemical vapor deposition, spray pyrolysis [10,11], sol–gel [12] and RF. magnetron sputtering [5] have been used to prepare ZnO films.

Recently, ZnO has attracted much attention as a new and promising electromagnetic wave-absorbing material due to its excellent dielectric properties. Sharma et al. had reported the effect of ZnO content on the dielectric properties of polyaniline–ZnO composite. The results indicated that the dielectric constant of polyaniline–ZnO composite was smaller than the polyaniline film, which was induced by the interfaces between ZnO particles and polyaniline [13,14]. Also, there has been reported on the optical properties of plasma sprayed ZnO/Al_2O_3 coatings [15]. Until now, however, there is no report on the dielectric properties at GHz frequencies of these coatings.

Atmospheric plasma spraying (APS) is an attractive technique for obtaining coatings and it has lots of advantages such as high achievable deposition efficiency, cost effectiveness and very specific coating properties. The high temperature of plasma spraying permits the deposition of coatings for applications in areas of engineering components and aircraft. Examples include protective layers to guard against high temperature, corrosion, abrasion and coatings used for electromagnetic shielding. In addition, due to the excellent mechanical properties, Al_2O_3 is widely used as the sprayed matrix of coatings. These coatings cover a wide range of materials including: Al_2O_3/ZrO_2 [16], Al_2O_3/TiO_2 [17,18], Al_2O_3/Al [19], Al_2O_3/Cr_2O_3 [20], Al_2O_3/SiC [21] etc. Therefore, in this paper, ZnO/Al_2O_3 composite coatings were fabricated by APS. The influence of ZnO content and annealing temperature on the microstructure, relative density and dielectric properties of the coatings were investigated systematically as a preliminary study for the application of ZnO/Al_2O_3 as electromagnetic wave absorbing coatings.

2. Experimental

2.1. Spray powder preparation

Commercial ZnO powder (≥99.0 wt%; D50 = 9 μm) and α-Al_2O_3 powder (>99.9 wt%; D50 = 0.8 μm) were used as starting raw materials. Composition of the samples can be found in Table 1. The starting raw materials were milled together for 1 h by planetary milling using agate ball and ethanol as a medium, and then

* Corresponding author. Tel.: +86 029 88494574; fax: +86 029 88494574.
E-mail address: zhouliang83@163.com (L. Zhou).

0925-8388/$ – see front matter.
doi:10.1016/j.jallcom.2011.03.018

Table 1
The sample codes and the component of the starting powders.

Sample codes	ZnO content (mol.%)	Al_2O_3 content (mol.%)	Annealing conditions	
			Temperature (°C)	Time (h)
A1	50	50	0	0
A2	55	45	0	0
A3	60	40	0	0
A4	65	35	0	0
A5	70	30	0	0
B5	70	30	400	10
C5	70	30	700	10

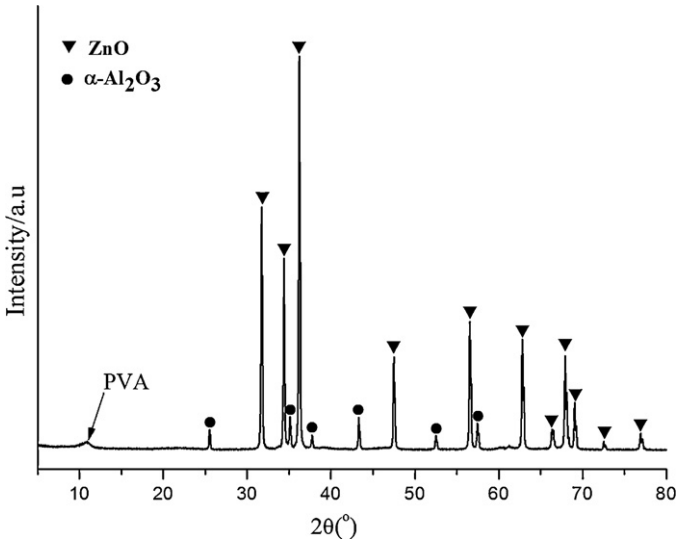

Fig. 1. X-ray diffraction pattern of starting ZnO/Al_2O_3 powders.

Table 2
Plasma spraying parameters.

Parameters	Value
Arc current, A	240
Arc voltage, V	35
Primary gas ($Ar + N_2$) flow rate, slpm	14
Secondary gas (N_2) flow rate, slpm	2
Spray distance, mm	110
Powder carrier gas flow rate, slpm	4
Powder feed rate, g/min	3

agglomerated with PVA as binder. After oven-dried at 100 °C for 2 h, the resulting mixtures were ground and passed through a sieve to acquire an appropriate particle size range for plasma spraying. The phase structure of the powder feedstock is shown in Fig. 1, The XRD pattern shows that ZnO and Al_2O_3 powders are composed of crystalline phases. And PVA is composed of one broadened peak with diffraction angle "2θ" ranging from 10° to 12°.

2.2. Plasma spraying

The coatings were fabricated by a commercial plasma spraying system with Ar and N_2 as plasma gases at a flow rate of 14 and 2 standard liters per minute (slpm), respectively. More details about the spraying parameters are listed in Table 2. The coatings were sprayed about 3.5 mm in thickness on graphite substrates. After deposition, they were mechanically removed from the substrates. To investigate the effect of annealing temperature on the dielectric properties of coatings, the freestanding coatings were finally annealed at 400 and 700 °C for 10 h in air using an electrical resistance furnace, with the heating rate of 10 K/min.

2.3. Characterization

The relative densities of the samples were measured using Archimedes method. The phase structure of the feedstock and the coatings was identified by X-ray diffraction (D/MAX2500 diffractometer) with Cu-Kα radiation. The scanning electronic microscope (JEOL JSM-6360LV) was used to reveal the microstructure of the coatings. The testing specimens were cut into rectangular blocks with dimensions of 10.16 mm (width) × 22.86 mm (length) × 2 mm (thickness) for the measurement of dielectric properties. The dielectric parameters were determined by E8362B PNA network analyzer with wave guide method in the frequency range of 8.2–12.4 GHz.

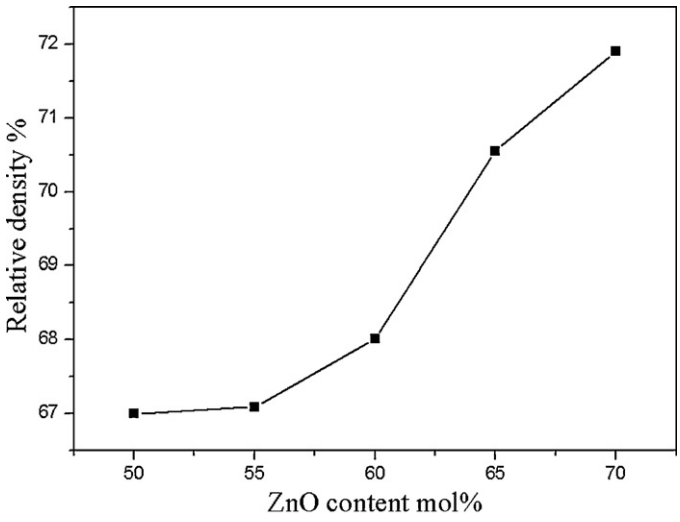

Fig. 2. The density of ZnO/Al_2O_3 composite coatings.

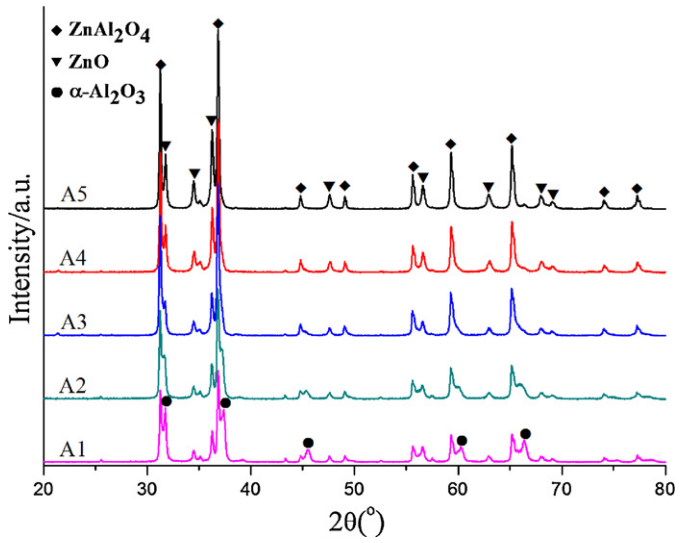

Fig. 3. X-ray diffraction pattern of as-sprayed coatings with different ZnO content.

3. Results and discussion

3.1. Relative density

The degree of melting of the particles affects the formation of the spherical liquid droplet and determines relative density of the coatings. The relative density of the coatings with different ZnO content is demonstrated in Fig. 2. It can be seen that the relative density of the coatings increases from 69.00% to 71.90% as the ZnO content increases from 50 to 70 mol.%. Owing to the low melting point, ZnO particles can be well melted during spraying, which results in the lower porosity of the samples with higher ZnO content.

3.2. Crystalline phase

The X-ray diffraction patterns of as-sprayed ZnO/Al_2O_3 coatings with different ZnO content are shown in Fig. 3. Fig. 4 shows XRD patterns of as-sprayed coatings with different ZnO content in the

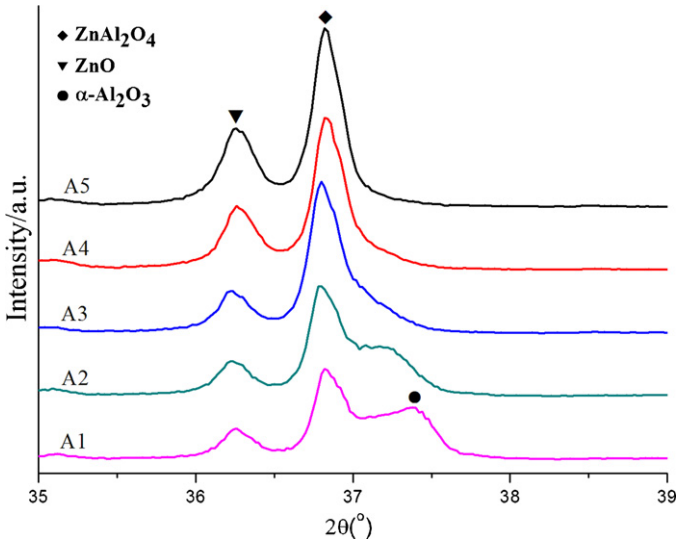

Fig. 4. X-ray diffraction pattern of as-sprayed coatings with different ZnO content in the 2θ range of 35–39.

2θ range of 35–39°. It can be seen that all the coatings are composed of ZnO, α-Al_2O_3 and $ZnAl_2O_4$, which means that a certain amount of ZnO and Al_2O_3 is turned into $ZnAl_2O_4$ due to the reaction between ZnO and Al_2O_3 in the spraying process. This result is in accordance with the previous report by Tului et al. [15]. At the same time, it can be shown from Fig. 4 that the ZnO and $ZnAl_2O_4$ peaks become higher with increasing ZnO content on the whole. In addition, when the ZnO content >60 mol.%, Al_2O_3 peaks can not be observed. This result reveals that Al_2O_3 has completely reacted with ZnO, resulting in more ZnO remained in the coatings.

As dielectric properties of ZnO/Al_2O_3 coating are very sensitive to ZnO content in the coatings, we measured the XRD patterns of coatings with 30% Al_2O_3 annealed at 0, 400 and 700 °C. From the XRD patterns of the annealed coatings with different annealing temperatures shown in Fig. 5, we can observe that all the samples contain ZnO and $ZnAl_2O_4$. Furthermore, as the annealing temperature increases from 0 to 700 °C, the intensity of ZnO diffraction peaks increases first and then decreases dramatically. While the ZnO diffraction peaks of the coating annealed at 400 °C are largest. This result indicates that the crystallinity of the coating is improved as the annealed temperatures increase, but higher annealing temperature leads to the decrease of ZnO content in the composite coatings.

3.3. Morphology and EDX analysis of as-sprayed coatings

Fig. 6 shows the surface morphology and EDX elemental analysis of ZnO/Al_2O_3 coating with 70 mol.% ZnO. Pores and microcracks can be observed clearly, which may be induced by shrinkage on cooling from the liquid state of the molted particles and the entrainment of air in the deposit, respectively. To differentiate ZnO and $ZnAl_2O_4$, an electron dispersive elemental analysis was carried out by EDS unit attached with SEM. According to the elemental analyses, the dark grey color represents the $ZnAl_2O_4$ matrix and the light grey color is the ZnO in the picture. The scanning electron micrographs confirm that networks are formed with the $ZnAl_2O_4$ matrix. Unreacted ZnO has undergone dissolution in the liquid particles when experienced high temperature in the spraying process, surrounding around the $ZnAl_2O_4$ matrix. It is noteworthy that some unmelted ZnO particles are embedded in the melted networks, due to their lower thermal conductivity.

3.4. Dielectric properties

3.4.1. Effect of ZnO content on dielectric properties

Fig. 7 illustrates the real (ε') part of the dielectric constant and the loss tangent factor ($\tan\delta = \varepsilon''/\varepsilon'$) in the frequency range of 8.2–12.4 GHz for the ZnO/Al_2O_3 composite coatings. As shown in Fig. 7, with the ZnO content increased from 50 to 70 mol.%, both the ε' and $\tan\delta$ increase greatly with increasing ZnO content across the whole frequency range. It also can be seen that, the ε' trends to decrease with increasing frequency and shows frequency dependence in the whole frequency range (8.2–12.4 GHz).

Generally, the dielectric properties of conductive particle filled insulation composites depends on the characteristics of the matrix, the property and volume fraction of the filler, the configuration of the composites, and the frequency of the electromagnetic wave

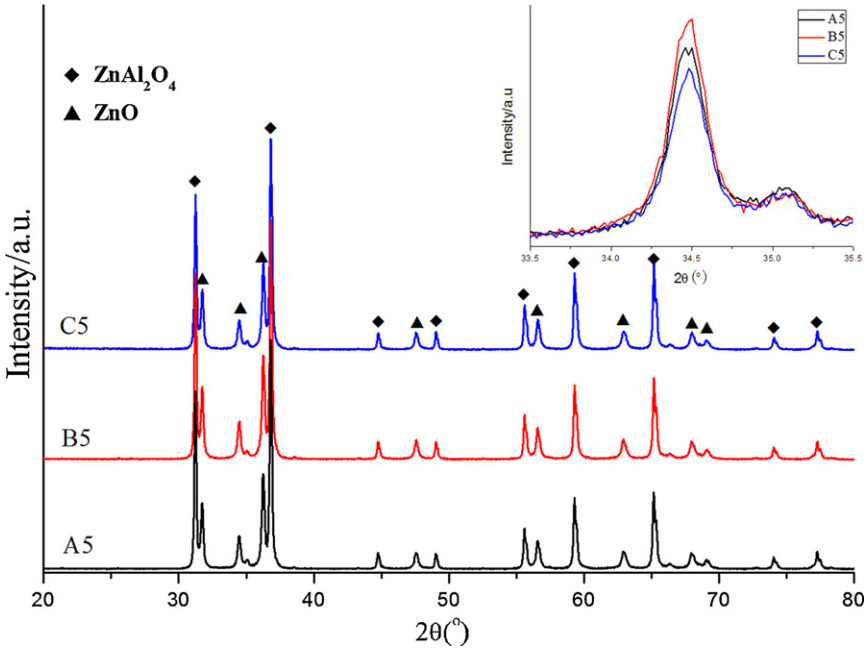

Fig. 5. X-ray diffraction pattern of coatings with 30% Al_2O_3 annealed at different temperature. The insert shows X-ray diffraction pattern in the 2θ range of 33.5–35.5.

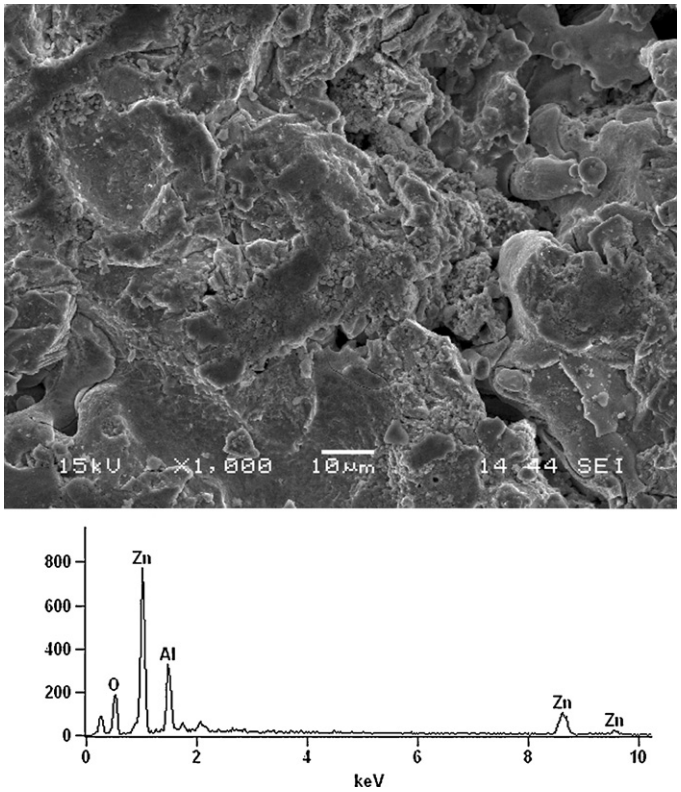

Fig. 6. SEM and EDX elemental analysis of cross-sectioned ZnO/Al_2O_3 coating with 70 mol.% ZnO.

[22,23]. It is well known that ZnO is a polar semiconductor [1,24]. Orientation polarization is an important polarization and associated relaxation will give rise to dielectric loss mechanism of ZnO/Al_2O_3 composite coatings. Moreover, the moving charge with alternating electrical field induced by relaxation polarization is also responsible for polarization and dielectric loss mechanisms of such composite coatings. Thus, it is considered that orientation polarization and relaxation polarization play roles in the complex permittivity of such composite coatings. It is reasonable that the higher ε' and $\tan\delta$ values can be obtained when the composite coatings are filled with a higher ZnO content, due to the higher orientation polarization and relaxation polarization of ZnO constituent.

According to the Debye theory [25,26], the relationship between ε' and frequency can be expressed as followed:

$$\varepsilon' = \varepsilon_\infty + \frac{\varepsilon_s - \varepsilon_\infty}{1 + \omega^2\tau(T)^2} \quad (1)$$

where ω is the angular frequency, ε_s is the static (zero frequency) permittivity, ε_∞ is the relative dielectric permittivity at high frequency limit and $\tau(T)$ represents the polarization relaxation time and it is related to temperature [27]. From Eq. (1), the $\omega\tau$ values increased with increasing the angular frequency. Thus, the frequency dispersion of ε' occurred as mentioned above.

On the other hand, it is observed that the $\tan\delta$ values increase with frequency to maximum value at 10 GHz and then decrease in higher frequency region as shown in Fig. 7(b). The dielectric loss ($\tan\delta$) could be explicated by Debye theory:

$$\tan\delta = \frac{\varepsilon''}{\varepsilon'} = \frac{(\varepsilon_s - \varepsilon_\infty)\omega\tau}{\varepsilon_s + \varepsilon_\infty\omega^2\tau^2} \quad (2)$$

Based on Eq. (2), the dielectric loss ($\tan\delta$) related to free dipoles oscillating in alternating electrical field could be described in the following way. At the low frequencies ($\omega < 1/\tau$), the relaxation time is large compared to the period of the applied field, losses are small. At high frequencies ($\omega > 1/\tau$) the relaxation process is rapid compared to the frequency of the applied, losses are also small. However, when the period of the relaxation process is the same as the period of the applied field ($\omega = 1/\tau$), the dielectric loss reached maximum value, as shown in Fig. 7(b) [27]. Similar results have been reported by Tripathi et al. [28].

3.4.2. *Effect of annealing temperature on dielectric properties*

Coatings with different annealing temperature were prepared in order to study the effect of annealing temperature on dielectric properties. Three coatings with the same composition were annealed under 0, 400 and 700 °C for 10 h, respectively. The real part (ε') and loss tangent ($\tan\delta$) of these coatings are shown in Fig. 8. It is evident that the coating annealed at 400 °C has larger dielectric constant and loss tangent than the one without annealed. As discussed before, the ZnO diffraction peaks increase with increasing annealing temperature, which is favorable for increasing the ε' and $\tan\delta$ values due to the higher ZnO content in the coatings, as shown in Fig. 8. Furthermore, the increase of annealing temperature is useful for the changing of thermal contraction of the lattice and electron–phonon interactions, benefiting for relaxation polarization. However, the ε' and $\tan\delta$ decrease dramatically after annealed at 700 °C for 10 h, which is ascribed to the decrease of

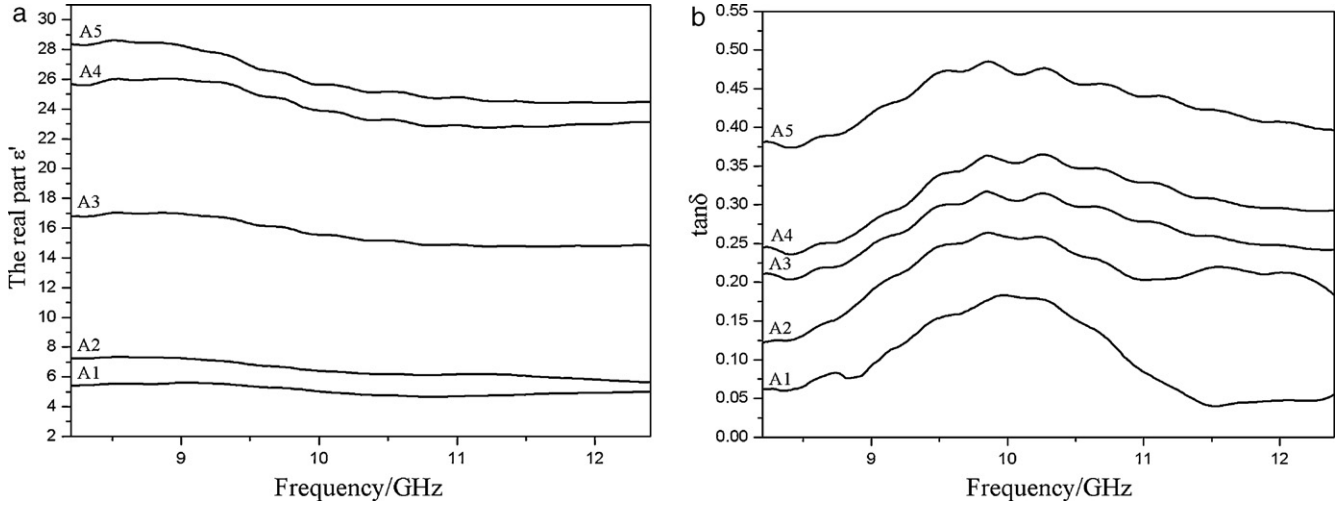

Fig. 7. (a) The real part (ε') and (b) the loss tangent ($\tan\delta$) of as-sprayed coatings versus frequency.

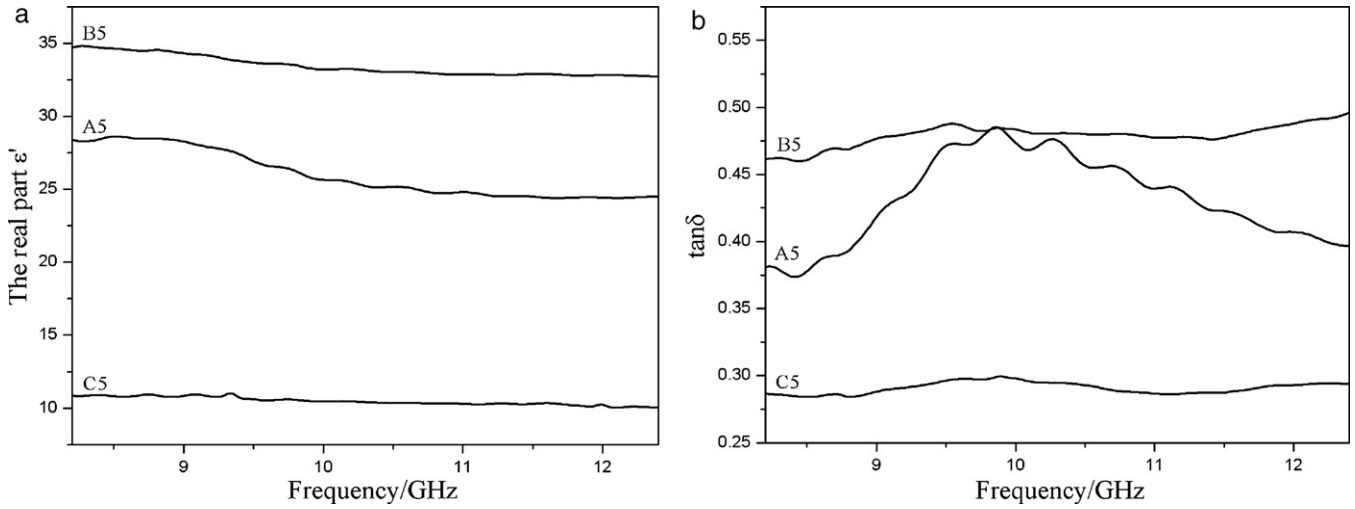

Fig. 8. (a) The real part (ε') and (b) loss tangent ($\tan\delta$) of annealed coatings of versus frequency.

polarization and associated relaxation induced by the decrease of ZnO content.

4. Conclusions

In this study, ZnO/Al_2O_3 powders were deposited onto graphite substrates to form coatings by APS spraying. The relative density of as-sprayed coatings increases from 69.00% to 71.90% as the ZnO content increases from 50 to 70 mol.%. The dielectric properties of coatings with different ZnO content were studied in detail in a frequency range of 8.2–12.4 GHz. The coatings with higher ZnO content present higher dielectric real part (ε') and loss tangent ($\tan\delta$), which are ascribed to orientation polarization and relaxation polarization. The frequency-dependent maximum of the loss tangent (tanδ) is found to obey Debye theory. In addition, annealing temperature also plays an important role in the dielectric performance. Proper annealing temperature induces the change of ZnO content, thermal contraction of the lattice and electron–phonon interactions in the composite coatings. Therefore, optimizing the dielectric properties through ZnO content and annealing temperature, ZnO/Al_2O_3 composite coatings are potentially employed in wave-absorbing field.

Acknowledgements

This work was supported by the fund of the State Key Laboratory of Solidification processing in NWPU, No. KP200901.

References

[1] Ü. Özgür, Ya.I. Alivov, C. Liu, et al., J. Appl. Phys. (2005) 041301.
[2] P. Ma, Y. Wu, Z. Fu, et al., J. Alloys Compd. 509 (2011) 3576–3581.
[3] Xiong Yu-Ying, Kang Feng, Ke Zheng, et al., J. Cryst. Growth 312 (2010) 2484–2488.
[4] R. Ye, S. Xu, D. Deng, et al., J. Lumin. 130 (2010) 2385–2389.
[5] D.K. Kim, H.B. Kim, J. Alloys Compd. 509 (2011) 421–425.
[6] A. Amlouk, K. Boubaker, M. Bouhafs, et al., J. Alloys Compd. 509 (2011) 3661–3666.
[7] M.H. Koch, P.Y. Timbrell, R.N. Lamb, Semicond. Sci. Technol. 10 (1995) 1523.
[8] J. Chen, J. Li, J. Li, et al., J. Alloys Compd. 509 (2011) 740–743.
[9] G. Zhu, T. Lv, L. Pan, et al., J. Alloys Compd. 509 (2011) 362–365.
[10] S.S. Shinde, P.S. Patil, R.S. Gaikwad, et al., J. Alloys Compd. 503 (2010) 416–421.
[11] T. Prasada Rao, M.C. Santhosh Kumar, J. Alloys Compd. 506 (2010) 788–793.
[12] L. Znaidi, Mater. Sci. Eng., B 174 (2010) 18–30.
[13] B.K. Sharma, A.K. Gupta, N. Khare, et al., Synth. Met. 159 (2009) 391.
[14] B.K. Sharma, N. Khare, S.K. Dhawan, et al., J. Alloys Compd. 477 (2009) 370.
[15] M. Tului, F. Arezzo, L. Pawlowski, Surf. Coat. Technol. 179 (2004) 47.
[16] Q. Yu, C. Zhou, H. Zhang, et al., J. Eur. Ceram. Soc. 30 (2010) 889–897.
[17] F. Vargas, H. Ageorges, P. Fournier, et al., Surf. Coat. Technol. 205 (2010) 1132–1136.
[18] C. Li, Y. Wang, L. Guo, et al., J. Alloys Compd. 506 (2010) 356–363.
[19] Z. Yin, S. Tao, X. Zhou, et al., Appl. Surf. Sci. 254 (2008) 1636.
[20] B.R. Marple, J. Voyer, P. Béchard, J. Eur. Ceram. Soc. 21 (2001) 861.
[21] S. Jiansirisomboon, K.J.D. MacKenzie, S.G. Roberts, et al., J. Eur. Ceram. Soc. 23 (2003) 961.
[22] E. Tuncer, Y.V. Serdyuk, S.M. Gubanski, IEEE Trans. Dielectrics Electrical Insulation 9 (October (5)) (2002).
[23] A.N. Lagarkov, A.K. Sarychev, Phys. Rev. B. 53 (1996) 6318–6336.
[24] Z. Dang, L. Fan, S. Zhao, et al., Mater. Res. Bull. 38 (2003) 499–507.
[25] M.-S. Cao, W.-L. Song, Z.-L. Hou, et al., Carbon 48 (2010) 788–796.
[26] J.E. Atwater, R.R. Wheeler Jr, Appl. Phys. A 79 (2004) 125–129.
[27] W.D. Kingery, H.K. Bowen, D.R. Uhlmann, Introduction to Ceramics, John Wiley, New York, 1976.
[28] R. Tripathi, A. Kumar, C. Bharti, et al., Curr. Appl. Phys. 10 (2010) 676–681.